Metastable zinc–nickel alloys deposited from an alkaline electrolyte

Luca Magagnin, Luca Nobili *, Pietro Luigi Cavallotti

Dip. Chimica, Materiali e Ing. Chimica Giulio Natta, Politecnico di Milano, Via Mancinelli 7, 20131 Milano, Italy

Available online 13 February 2014

1. Introduction

Sacrificial protection to steel provided by zinc coatings is well known. Zinc alloys dissolve more slowly than pure zinc and are frequently used on account of their longer duration, especially in the automotive industry. Zn–Ni coatings are reported to provide the best protective properties when they consist of a single-γ phase layer with a dense and homogeneous microstructure [1,2]. Deposition conditions are also important and the electrolytic bath used in this work can provide high-performance coatings. Thus, the investigation of their structural properties is stimulated.

Electrodeposited Zn–Ni coatings commonly exhibit phase compositions different from those predicted by the Zn–Ni phase diagram [3–5]. Similar disagreement is observed in many other electrodeposited alloys, typical deviations being represented by extended solubility, modified composition range of two-phase fields and absence of ordered intermetallic compounds.

In some systems, the phase composition of electrodeposited alloys can be predicted by analysing the free-energy curves of all the phases and calculating metastable equilibrium conditions by neglecting the ordered compounds [5]. However, the same expression for free energy is usually taken for the electrodeposited phase and the corresponding bulk phase, because the same crystalline structure is postulated for both phases.

* Corresponding author.
E-mail address: luca.nobili@polimi.it (L. Nobili).

In the present work, structural and thermodynamic properties of Zn–Ni coatings have been investigated. Insights into the atomic arrangement in electrodeposited alloys and its possible effects on coating performance can be derived from the results of this study.

2. Experimental methods

Zn–Ni alloy coatings were electrodeposited from a cyanide-free commercial bath. It is an alkaline solution containing zinc oxide, nickel sulphate, sodium hydroxide, complexing agent (amine) and proprietary additives. The operating temperature is 25 °C and the deposition rate is 0.3 μm/min at the current density of 2 A/dm^2.

Coatings with nickel content between 14 wt.% (15.4 at.%) and 17 wt.% (18.6 at.%) are deposited from this bath. Such coatings can achieve outstanding corrosion resistance, they can endure more than 1000 h of exposure in salt spray chamber without marks of red rust.

The nickel content was analysed by energy dispersive X-ray spectroscopy (EDS). Samples examined in this work have a nickel fraction of 17 wt.% (18.6 at.%), very close to the composition Ni_5Zn_{21} (19.2 at.%).

Crystalline structure was analysed by X-ray diffraction (XRD) experiments with a Cu Kα radiation. Coatings were tested in the as-deposited condition and after substrate removal and subsequent annealing in nitrogen for one hour at 400 °C.

Differential Scanning Calorimetry (DSC) was used to investigate the thermal stability of the substrate-free Zn–Ni coatings. The heating rate was 10 °C min^{-1}.

3. Results and discussion

On the Zn-rich side of the Zn–Ni system the equilibrium solid phases are: the solid solution with hexagonal close packed (hcp) structure and very small solubility of Ni (η phase), the monoclinic

δ phase (~10–11 at.% Ni) and the cubic γ phase (~15–26 at.% Ni) [6]. The composition limits between round brackets are valid up to about 400 °C (δ phase) and 500 °C (γ phase).

3.1. XRD and DSC results

The diffraction pattern of the as-deposited Zn–Ni coating with 17 wt.% (18.6 at.%) Ni is reported in Fig. 1a. The diffraction lines of this coating can be identified as reflections of the γ-Ni_5Zn_{21} phase (JCPDS card No. 6-0653) and no other phase can be recognized. Peaks labelled as "Fe" are given by the steel substrate. It should be noted that the peak at 34.95° is not identified and many high-intensity reflections of the γ-Ni_5Zn_{21} phase are not present in the XRD spectrum of the coating.

After the annealing treatment the diffraction pattern changes (Fig. 1b), the main difference being the increased number of reflection peaks. Substantially all the diffraction lines of the γ-Ni_5Zn_{21} phase are present in the spectrum of the annealed coating. Peaks labelled with letters "a"–"g" cannot be assigned to known phases in the Zn–Ni system and will be examined later.

The DSC thermogram exhibits three broad exothermic peaks centred around temperatures comprised in the range of 140–370 °C (Fig. 2). Similar DSC curves were obtained from Zn–Ni coatings with Ni content between 6.5 wt.% (7.2 at.%) and 13.5 wt.% (14.8 at.%) [3].

The modification of the diffraction spectrum after annealing and the enthalpy change measured by DSC analysis suggest that the atomic arrangement in the electrodeposited alloy can be different from the ordered atomic distribution existing in the equilibrium γ phase.

The symmetry of the γ phase is body-centred cubic and the structure can be described in terms of inner tetrahedral (4), outer tetrahedral (4), octahedral (6) and cubo-octahedral (12) positions, all centred around the origin and the body centre of the unit cell [7]. The number of atomic sites in each position is reported between round brackets. In the stable phase, Ni atoms occupy the outer tetrahedral positions yielding a structure with the minimum number of Ni–Ni contacts [7]. The higher enthalpy content of the electrodeposited phase suggests that Ni atoms can occupy all the sublattice positions with equal probability, rather than being confined to the outer tetrahedral sites. In this way, each Ni atom will be surrounded by a larger number of similar atoms, compared to the arrangement of the ordered γ phase.

X-ray structure factors and diffraction intensities were calculated for the γ structure with Ni atoms randomly distributed over all atomic sites and the calculated diffraction pattern is shown in Fig. 1c. All the peaks of the as-deposited alloy (Fig. 1a) correspond to diffraction lines of the calculated spectrum, including the reflection at 34.95°. In addition, all the peaks labelled with letters "a"–"g" in Fig. 1b can be assigned to the γ structure with random atomic distribution (Fig. 1c). Presumably these low-intensity peaks belong to the residual deposited alloy, which was not completely transformed during the annealing treatment. Only the most intense peak (letter "b") is visible in the diffraction spectrum of the as-deposited alloy, presumably because the other peaks are masked by the relatively intense background signal (Fig. 1a).

On the analogy of similar systems, the ordering transformation of the electrodeposited phase is expected to occur by a nucleation and growth mechanism or a continuous ordering reaction, according to the transformation temperature [8]. However, the atomic structure of the γ phase is relatively complex, as said above, and

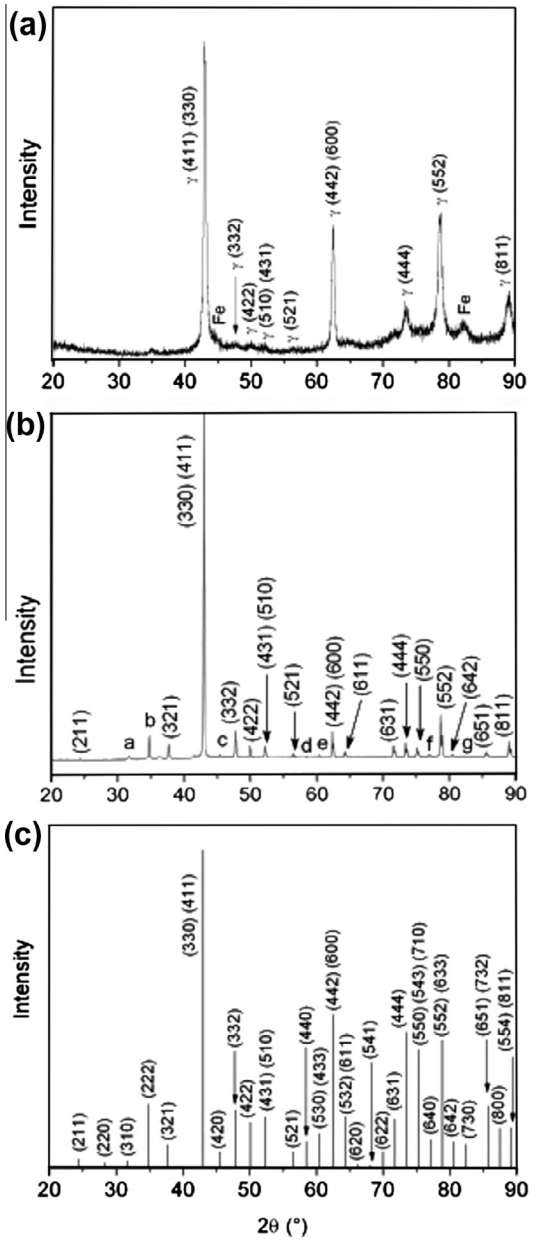

Fig. 1. XRD patterns of as-deposited (a) and annealed (b) Zn–Ni coatings; calculated XRD spectrum of a γ structure with randomly distributed Ni atoms (c).

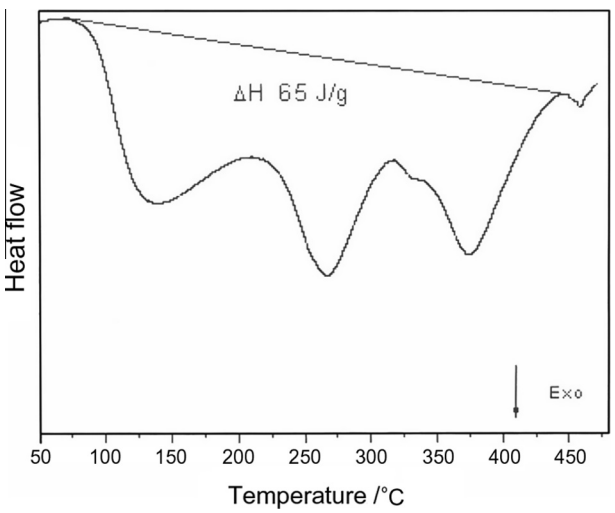

Fig. 2. DSC trace obtained from the Zn–Ni coating.

the ordering transformation of the Zn–Ni alloy would imply atomic rearrangement over several sublattices. The transformation might occur through a single stage or the atomic redistribution might proceed by involving different sublattices step by step. Further investigation is required to elucidate these features and to correlate the transformation steps to the exothermic peaks in the DSC trace.

The possible contribution of grain growth to the enthalpy change measured by DSC analysis was estimated from line broadening in the XRD spectra. By using the Scherrer equation, the average crystallite size was found to be 34 nm in the as-deposited alloy and increased to 61 nm after annealing. An enthalpy change of −0.11 kJ/mol was evaluated by employing experimental values of grain boundary energy in zinc [9]. This rough calculation shows that grain growth represents a small part of the total enthalpy change (−4.2 kJ/mol).

3.2. Thermodynamic evaluation

Thermodynamic assessment of the Ni–Zn system has been performed by making use of different sublattice models for the γ phase [10–12]. The model proposed by Su et al. [11] was selected to calculate the Gibbs free energy for the electrodeposited phase, because it is based on experimental crystallographic data [7]. These data are necessary to construct the calculated XRD pattern shown in Section 3.1 and were actually used to this purpose.

The equilibrium γ phase is described by the three-sublattice model $(Ni,Zn)_4Ni_4Zn_{18}$, where the inner tetrahedral sites can be occupied by Ni atoms and Zn atoms [11]. The other positions are occupied by Ni atoms only (outer tetrahedral sites) or Zn atoms only (octahedral and cubo-octahedral sites). As a result, the composition range is between Ni_4Zn_{22} and Ni_8Zn_{18}.

The electrodeposited alloy was described as a regular solution, on account of the random atomic distribution discussed in Section 3.1. At the given composition (18.6 at.% Ni), the enthalpy of mixing ($\Delta H^{ed\text{-}\gamma}$) was estimated by the equation

$$\Delta H^{ed\text{-}\gamma} = \Delta H^{\gamma} - \Delta H_{DSC} \quad (1)$$

where ΔH_{DSC} is the enthalpy change measured by DSC (-4.2 kJ/mol) and ΔH^{γ} is the enthalpy of mixing of the equilibrium γ phase. This quantity was derived from the free energy function reported in [11]. Accordingly, the expression of the molar Gibbs free energy for the electrodeposited phase becomes

$$G^{ed-\gamma} = x_{Ni}{}^{\circ}G^{bcc}_{Ni} + (1-x_{Ni}){}^{\circ}G^{bcc}_{Zn} + RT[x_{Ni}\ln(x_{Ni}) + (1-x_{Ni})\ln(1-x_{Ni})] + Wx_{Ni}(1-x_{Ni}) \quad (2)$$

where x_{Ni} is the atomic fraction of nickel, R is the gas constant and T is the absolute temperature. The Gibbs free energy of the pure elements ($^{\circ}G^{bcc}_{Ni}$, $^{\circ}G^{bcc}_{Zn}$) is calculated from the SGTE data set [13].

The interaction parameter is $W = -100.3$ kJ/mol. The negative value of this parameter confirms that the enthalpy of mixing decreases as the number of Ni–Zn pairs (proportional to the product $x_{Ni}x_{Zn}$) increases. The Gibbs free energy for the equilibrium γ phase is expressed according to a pair-wise interaction model [11]. The interaction parameter is negative in this phase too. At the composition Ni_4Zn_{22}, Ni atoms occupy the outer tetrahedral sites and form Ni–Zn pairs only, because they are surrounded by atoms belonging to the other sublattices, which contain Zn atoms only. As the Ni content increases, Zn atoms are replaced by Ni atoms in the inner tetrahedral positions and the number of Ni–Zn pairs becomes larger. In the disordered phase, Ni atoms are randomly distributed in all sublattices and the total number of Ni–Zn pairs decreases compared to the ordered phase with the same composition. Therefore, the transition from the electrodeposited phase to the stable intermetallic compound will cause the number of Ni–Zn pairs to increase and will produce a negative enthalpy change, in agreement with the DSC analysis.

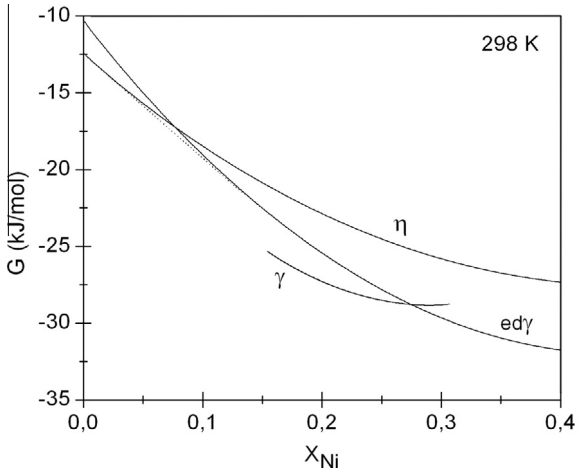

Fig. 3. Molar Gibbs free energy at 298 K as a function of the nickel atomic fraction for different phases: hcp solid solution (η), equilibrium γ phase (γ) and electrodeposited γ phase (ed-γ). The common tangent between η and edγ is shown as a dotted line.

Free energy curves at 298 K are reported in Fig. 3. This plot shows that the metastable equilibrium between the hcp solid solution (η) and the electrodeposited γ phase (edγ) entails the existence of η from 0 to 1.5 at.% Ni, η + edγ from 1.5 to 13.5 at.% Ni and edγ at higher Ni content. This prediction is in agreement with experimental results about the electrodeposition of Zn–Ni alloys with different composition [2,14–17]. According to these results, the upper limit of the η + γ field can be the range 11–15 at.% Ni. Such variability can be due to the different deposition conditions, which may influence features of the coating like uneven solute distribution [15], incorporation of impurities or grain boundary area [5]. The calculated phase boundary (13.5 at.%) is affected by the experimental error in ΔH_{DSC} and the approximate description of the thermodynamic properties (regular solution model). However, the quantitative agreement with the experimental range (11–15 at.%) indicates that the approximation can be acceptable. It is also noted that the common tangent in Fig. 3 is hardly distinguished from the free energy curves of the two phases (η and edγ). Therefore, the occurrence of the single-γ phase in coatings with Ni content smaller than 13.5 at.% would entail a very small increase in free energy, with respect to the two-phase system (η + edγ). This remark would explain the presence of the single-γ phase in Zn–Ni coatings with Ni content ranging from 8 wt.% (8.8 at.%) to 16 wt.% (17.5 at.%) [18].

4. Conclusions

Zn–Ni alloys with single γ phase were deposited from an alkaline electrolytic bath. XRD and DSC results show that the electrodeposited phase exhibits different atomic distribution and enthalpy content compared with the equilibrium γ compound.

The electrodeposited phase was described as a random distribution of Ni atoms over the sublattice positions of the γ structure. The diffraction pattern of this phase was calculated and provided a satisfactory interpretation of the diffraction spectra of the as-deposited and annealed alloys.

The Gibbs free energy of the electrodeposited phase was evaluated and the metastable phase boundaries were obtained. Reasonable agreement was found with experimental values reported in the literature.

This work provides new insights into atomic arrangement of electrodeposited alloys and can be extended to other systems, especially those which present ordered intermetallic compounds in their phase diagram.

Acknowledgements

The authors are grateful to Glomax srl for providing the commercial ZnNi electrolyte and to Prof. Livio Battezzati for performing DSC measurements and useful discussions.

References

[1] A. Conde, M.A. Arenas, J.J. de Damborenea, Electrodeposition of Zn–Ni coatings as Cd replacement for corrosion protection of high strength steel, Corros. Sci. 53 (2011) 1489–1497.

[2] R. Fratesi, G. Roventi, Corrosion resistance of Zn–Ni alloy coatings in industrial production, Surf. Coat. Technol. 82 (1996) 158–164.

[3] C. Bories, J.-P. Bonino, A. Rousset, Structure and thermal stability of zinc–nickel electrodeposits, J. Appl. Electrochem. 29 (1999) 1045–1051.

[4] Bruet-Hotellaz, J.P. Bonino, A. Rousset, Marolleau, E. Chauveau, Structure of zinc–nickel alloy electrodeposits, J. Mater. Sci. 34 (1999) 881–886.

[5] P.L. Cavallotti, L. Nobili, A. Vicenzo, Phase structure of electrodeposited alloys, Electrochim. Acta 50 (2005) 4557–4565.

[6] T.B. Massalski (Ed.), Binary Alloy Phase Diagrams, American Society for Metals, Metals Park, OH, 1986.

[7] A. Johansson, H. Ljung, S. Westman, X-Ray and neutron diffraction studies on Γ-Ni,Zn and Γ-Fe,Zn, Acta Chem. Scand. 22 (1968) 2743–2753.

[8] R.D. Doherty, Diffusive phase transformations in the solid state, in: R.W. Cahn, P. Haasen (Eds.), Physical Metallurgy, vol. 2, fourth ed., North-Holland, Amsterdam, 1996, pp. 1490–1494.

[9] D.A. Molodov, C. Günster, G. Gottstein, L.S. Shvindlerman, A novel experimental approach to determine the absolute grain boundary energy, Philos. Mag. 92 (2012) 4588–4598.

[10] G.P. Vassilev, T. Gomez-Acebo, J.-C. Tedenac, Thermodynamic optimization of the Ni–Zn system, J. Phase Equilib. 21 (2000) 287–301.

[11] X. Su, N.-Y. Tang, J.M. Toguri, Thermodynamic assessment of the Ni–Zn system, J. Phase Equilib. 23 (2002) 140–148.

[12] W. Xiong, H. Xu, Y. Du, Thermodynamic investigation of the galvanizing systems, II: thermodynamic evaluation of the Ni–Zn system, CALPHAD 35 (2011) 276–283.

[13] A.T. Dinsdale, SGTE data for pure elements, CALPHAD 15 (1991) 317–425.

[14] G. Barcelo, E. Garcia, M. Sarret, C. Muller, J. Pregonas, Characterization of zinc–nickel alloys obtained from an industrial chloride bath, J. Appl. Electrochem. 28 (1998) 1113–1120.

[15] T.V. Byk, T.V. Gaevskaya, L.S. Tsybulskaya, Effect of electrodeposition conditions on the composition, microstructure, and corrosion resistance of Zn–Ni alloy coatings, Surf. Coat. Technol. 202 (2008) 5817–5823.

[16] G.Y. Li, J.S. Lian, L.Y. Niu, Z.H. Jiang, Investigation of nanocrystalline zinc–nickel alloy coatings in an alkaline zincate bath, Surf. Coat. Technol. 191 (2005) 59–67.

[17] J. Giridhar, W.J. van Ooij, Study of Zn–Ni and Zn–Co alloy coatings electrodeposited on steel strips, Surf. Coat. Technol. 52 (1992) 17–30.

[18] C.S. Lin, H.B. Lee, S.H. Hsieh, Microstructure and formability of ZnNi alloy electrodeposited sheet steel, Metall. Mater. Trans. A 31 (2000) 475–485.